Directed Iron-Catalyzed *ortho*-Alkylation and Arylation: Towards the Stereoselective Catalytic Synthesis of 1,2-Disubstituted Planar-Chiral Ferrocene Derivatives

David Schmiel and Holger Butenschön*

Institutfür Organische Chemie
Leibniz Universität Hannover
Schneiderberg 1B
D-30167 Hannover
Germany
ORCID ID: 0000-0002-7689-1992
holger.butenschoen@mbox.oci.uni-hannover.de
www.ak-butenschoen.uni-hannover.de

Supporting Information (SI)

Table of contents:

Diastereoselective *ortho*-lithiation of (*S*)-26

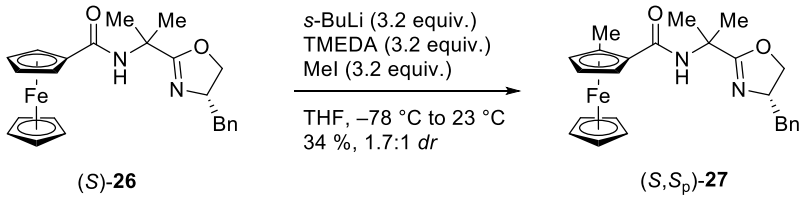

(*S*)-**26** (52 mg, 0.12 mmol) was dissolved in THF (2 mL), TMEDA (60 µL, 0.4 mmol) was added, and the mixture was cooled to –78 °C. Then, *s*-BuLi [1.3 M in cyclohexane/hexane (92/8), 0.3 mL, 0.4 mmol) was added dropwise and the mixture was stirred at –78 °C for 2 h. After the addition of methyl iodide (20 µL, 0.4 mmol), the mixture was heated to 23 °C. Then, sat. aq. NH_4Cl (3 mL) was added. The aqueous layer was extracted with ethyl acetate (5 mL). The combined organic layers were washed with brine (5 mL), dried with $MgSO_4$, filtered and concentrated at reduced pressure. Column chromatography (25 x 5 cm; petroleum ether/ethyl acetate 2:1) affored (S,S_p)-**27** (18 mg, 0.04 mmol, 34 %, 1.7:1 *dr* determined by ^{1}H-NMR) as an orange oil.

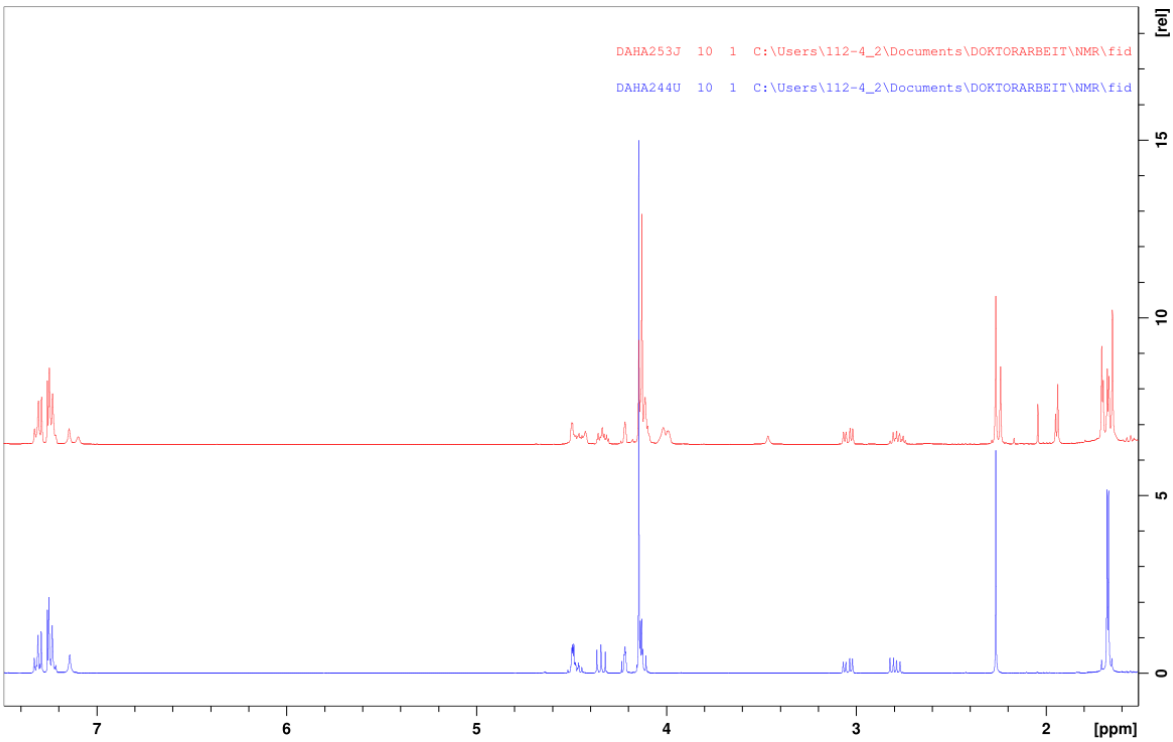

Figure S1. ^{1}H NMR spectra of (S,S_p)-**27** and comparison of *ortho*-lithiation (red) with *ortho*-C-H activation (blue)

Figure S2. ^{1}H (400 MHz) and ^{13}C (100.6 MHz) NMR Spectra of *N*-(8-Quinolinyl)-2-benzyl-ferrocenoylamide (*rac*-**2**) in [D_6]acetone

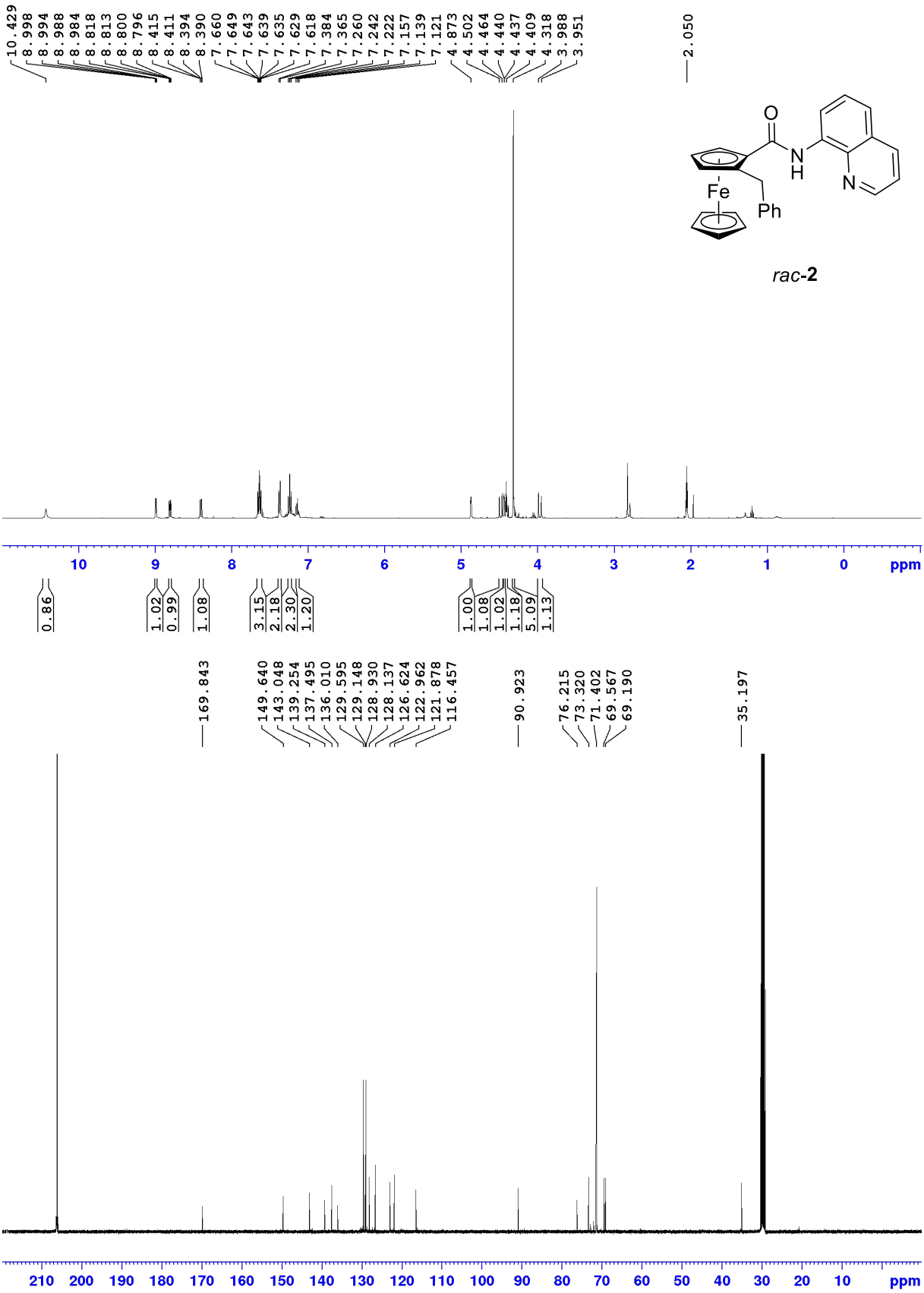

Figure S3. ^{1}H (400 MHz) and ^{13}C (100.6 MHz) NMR Spectra of *N*-(8-Quinolinyl)-2-phenyl-ferrocenoylamide (*rac*-**3**) in $CDCl_3$

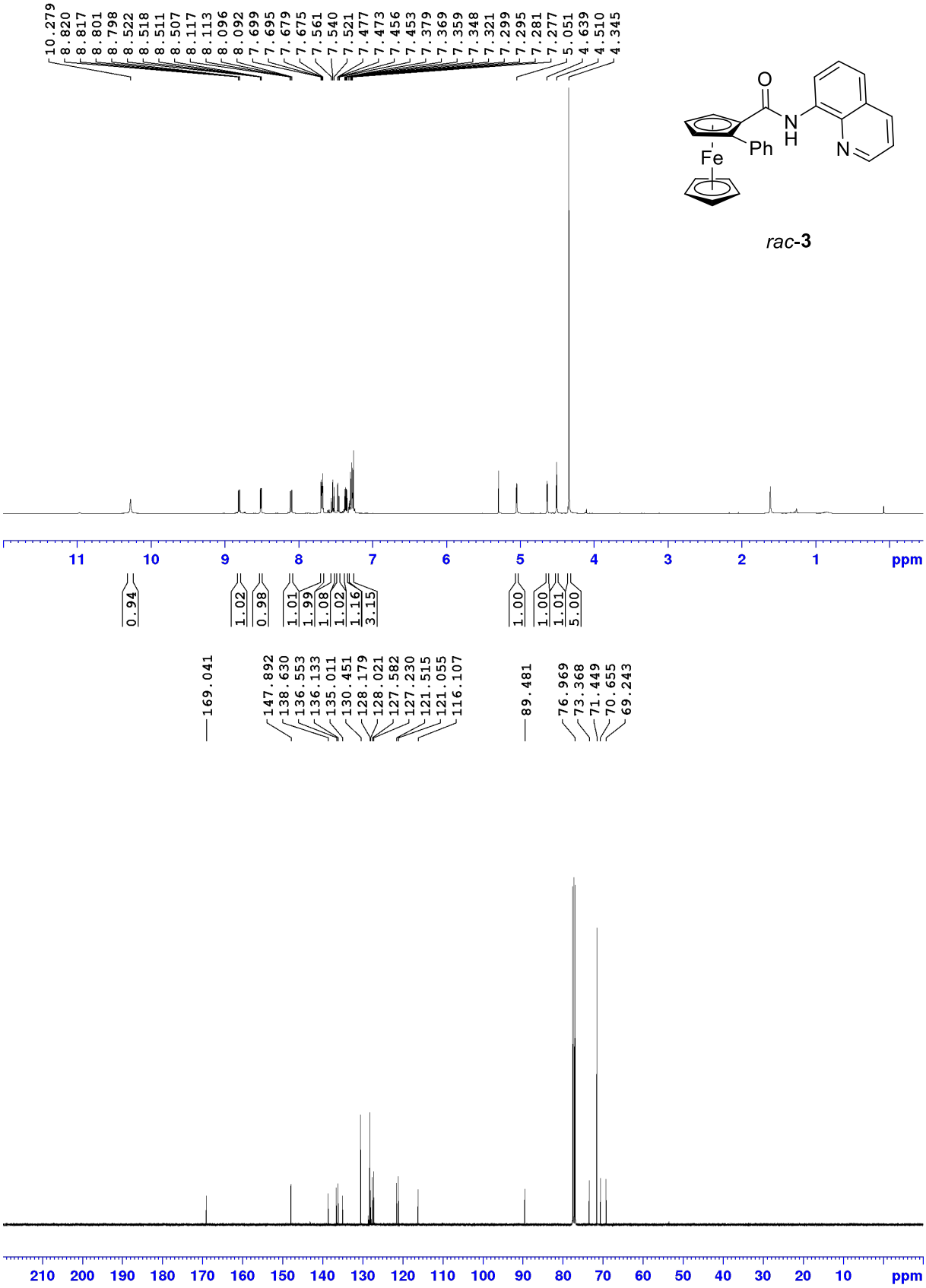

Figure S4. ^{1}H (400 MHz) and ^{13}C (100.6 MHz) NMR Spectra of *N*-[2-(1-Benzyl-1*H*-1,2,3-triazol-4-yl)-propan-2-yl]-2-phenylferrocenoylamide (*rac*-**6**) in $CDCl_3$

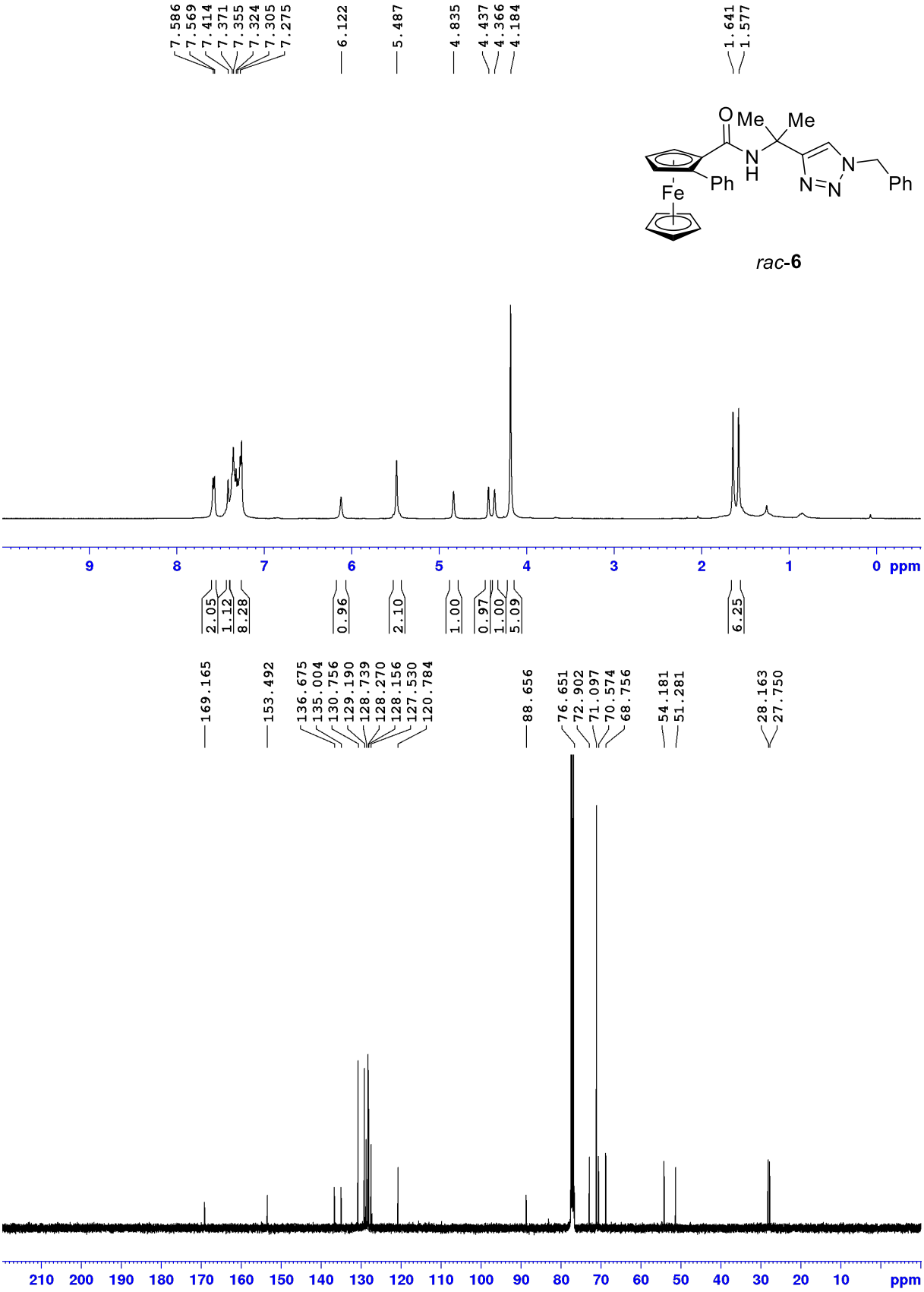

Figure S5. ^{1}H (400 MHz) and ^{13}C (100.6 MHz) NMR Spectra of *N*-[2-(1-Benzyl-1*H*-1,2,3-triazol-4-yl)-propan-2-yl]-2,5-diphenylferrocenoylamide (**7**) in $CDCl_3$

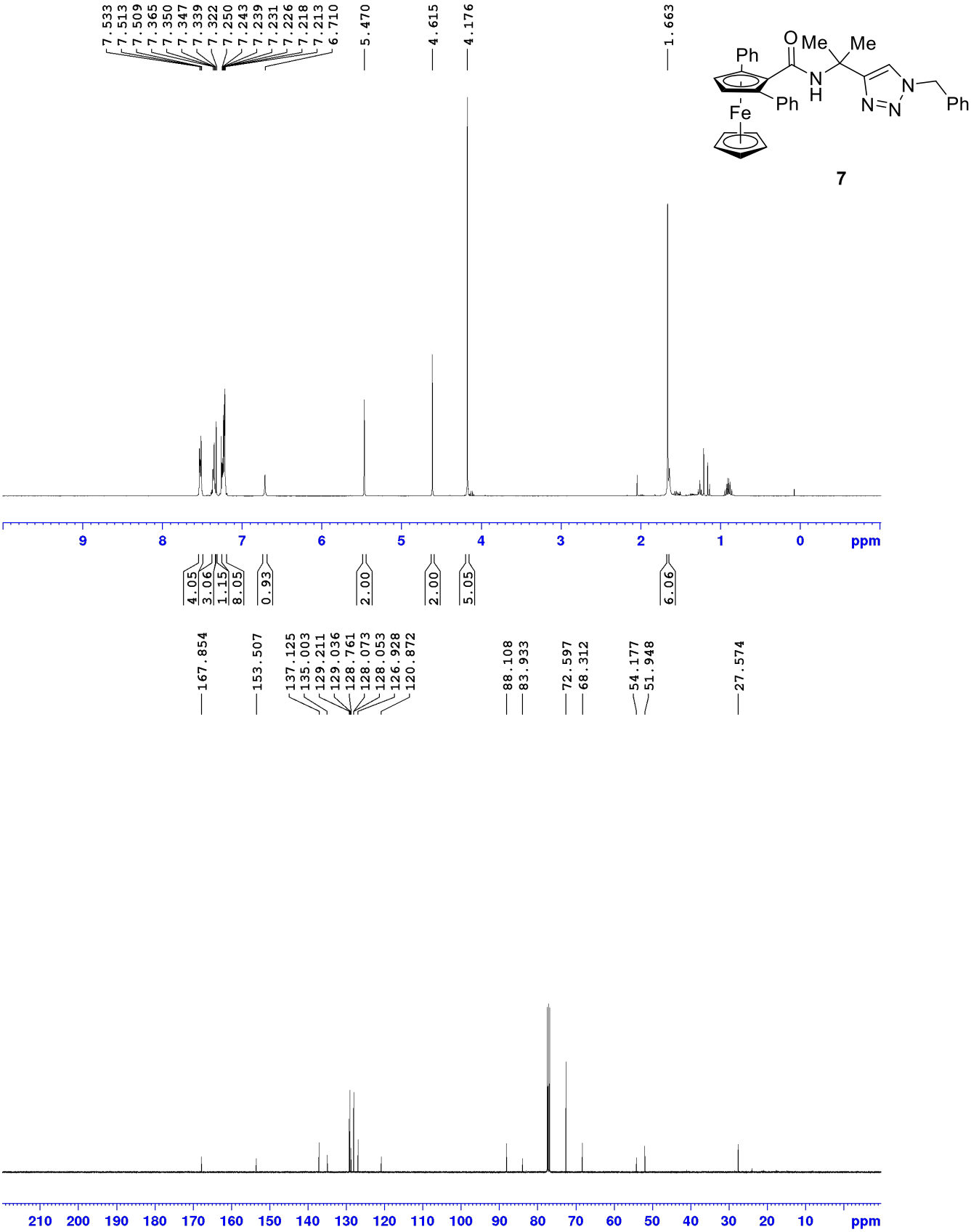

Figure S6. ^{1}H (400 MHz) and ^{13}C (100.6 MHz) NMR Spectra of *N*-[2-(2-Pyridyl)propan-2-yl]-ferrocenoylamide (**8**) in $CDCl_3$

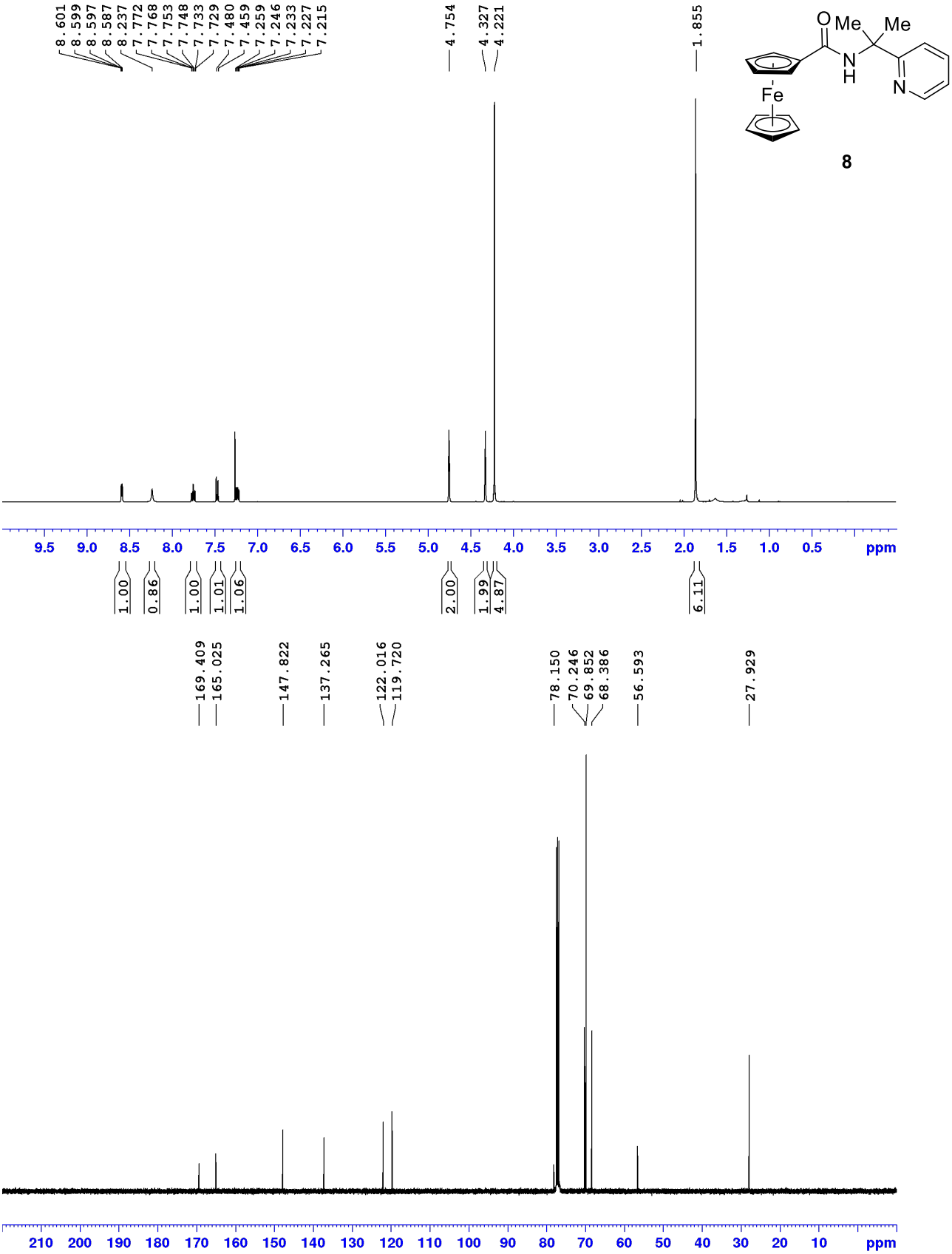

Figure S7. ^{1}H (400 MHz) and ^{13}C (100.6 MHz) NMR Spectra of *N*-[2-(2-Pyridyl)propan-2-yl]-2-phenylferrocenoylamide (*rac*-**9**) in $CDCl_3$

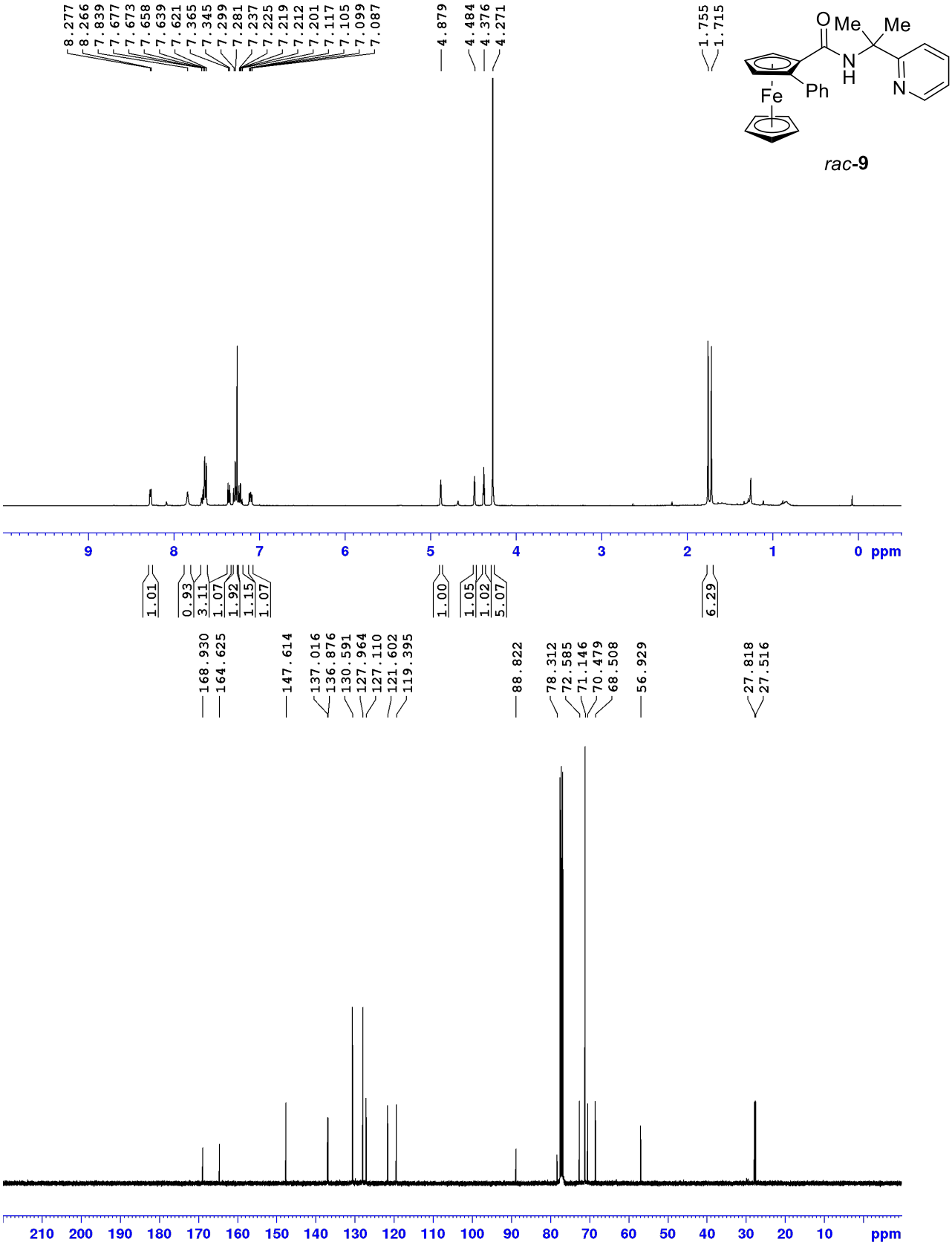

Figure S8. ^{1}H (400 MHz) and ^{13}C (100.6 MHz) NMR Spectra of *N*-(8-Quinolinyl)-2-(4-methyl-phenyl)ferrocenoylamide (*rac*-**10**) in $CDCl_3$

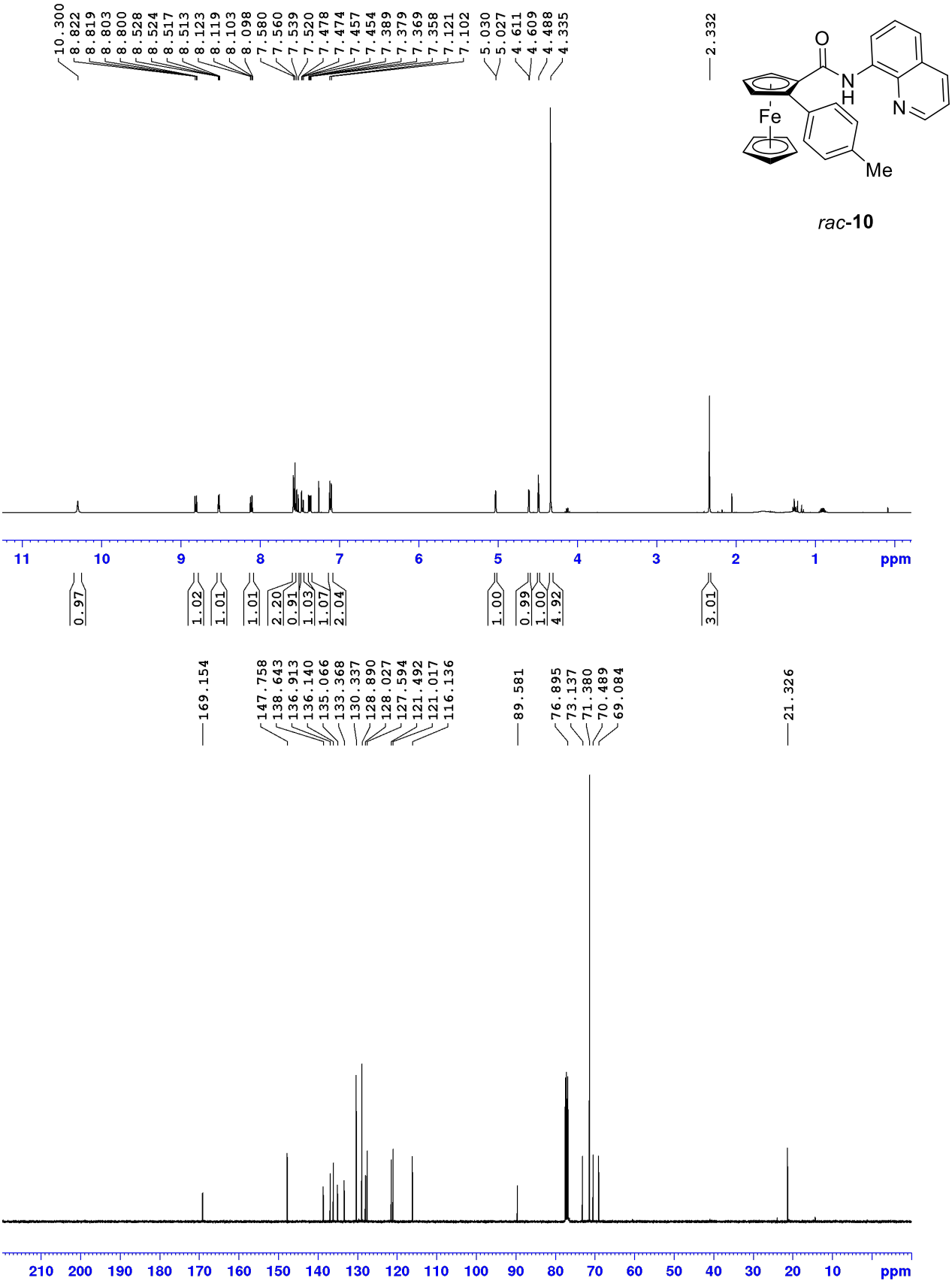

Figure S9. ^{1}H (400 MHz) and ^{13}C (100.6 MHz) NMR Spectra of *N*-(8-Quinolinyl)-2-(4-trifluoromethylphenyl)ferrocenoylamide (*rac*-**11**) in $CDCl_3$

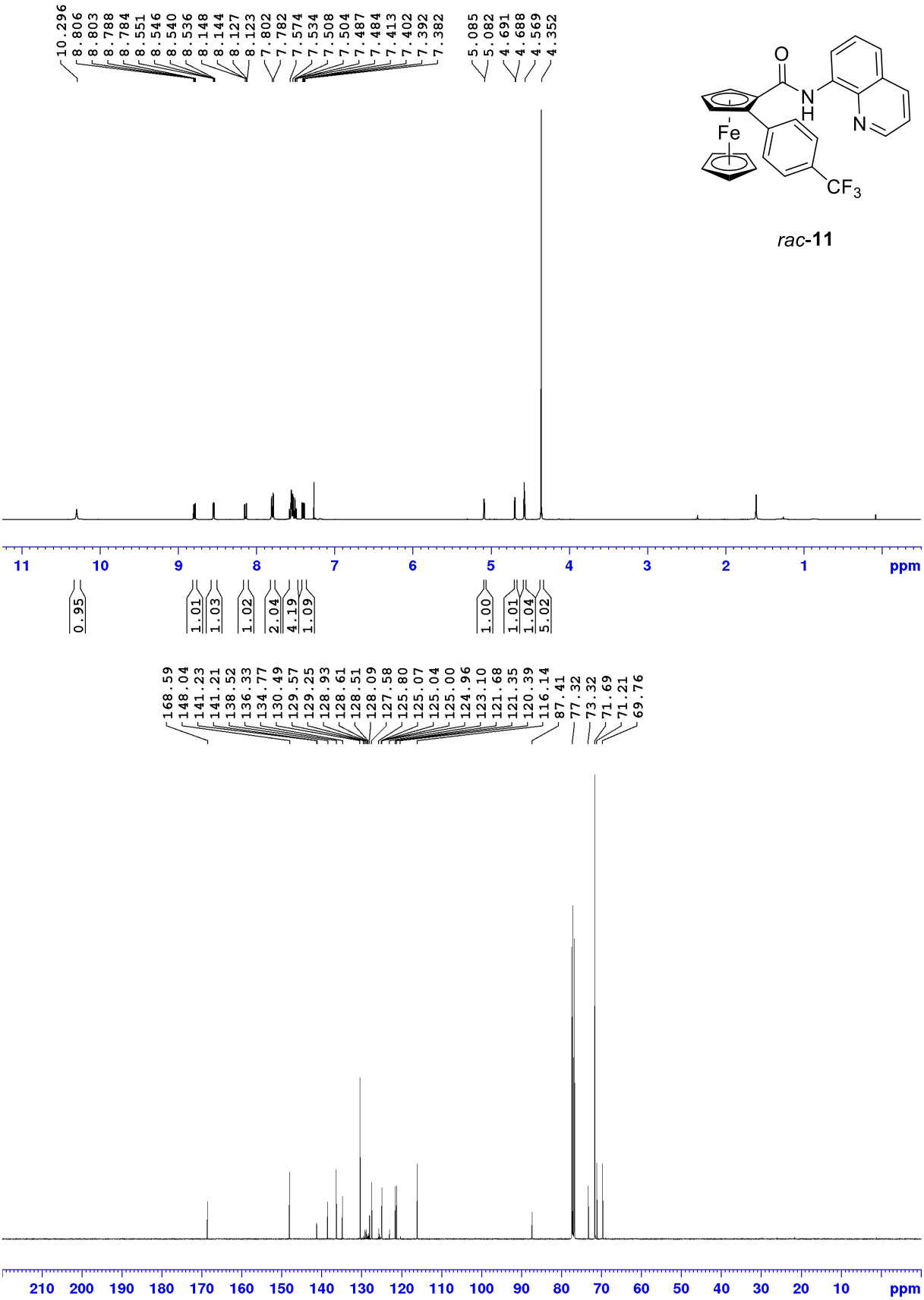

Figure S10. ^{19}F (376.5 MHz) NMR Spectrum of *rac*-**11** in $CDCl_3$

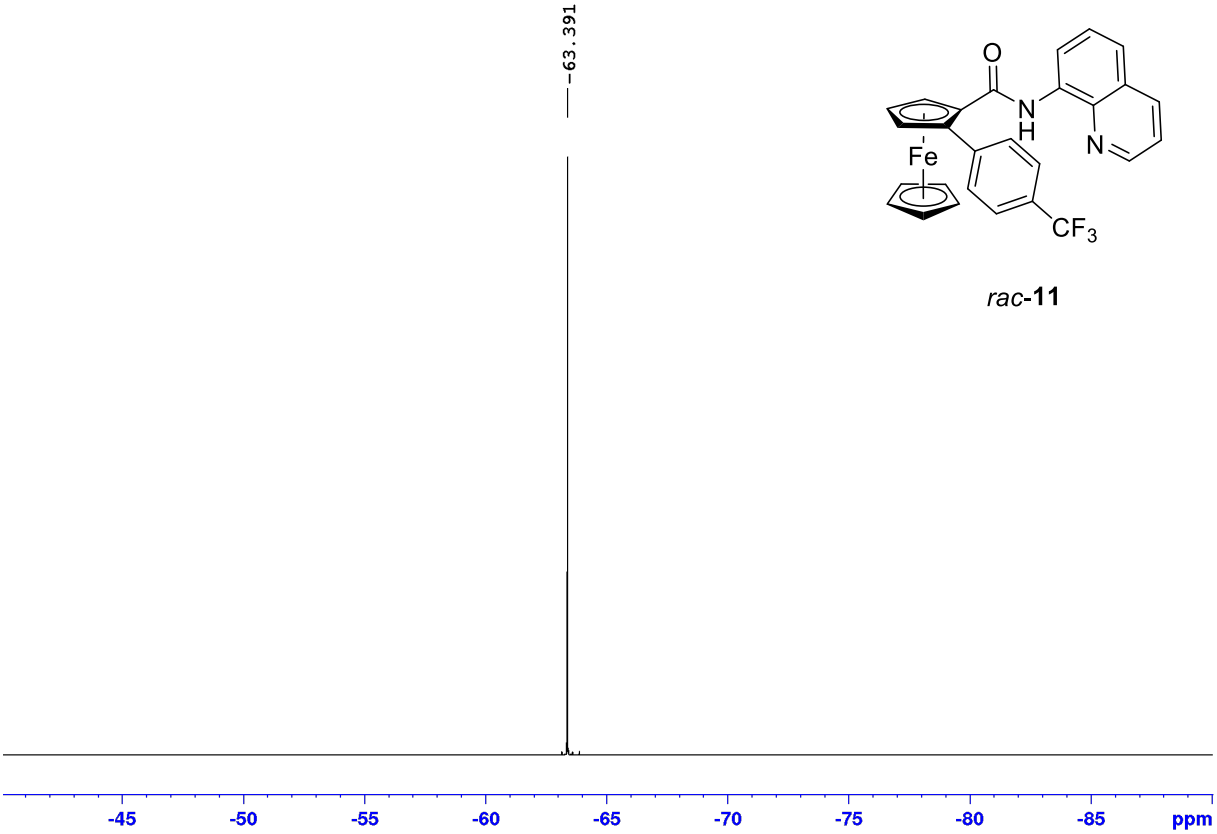

Figure S11. ^{1}H (400 MHz) and ^{13}C (100.6 MHz) NMR Spectra of *N*-(8-Quinolinyl)-2-(4-methoxy-phenyl)ferrocenoylamide (*rac*-**12**) in $CDCl_3$

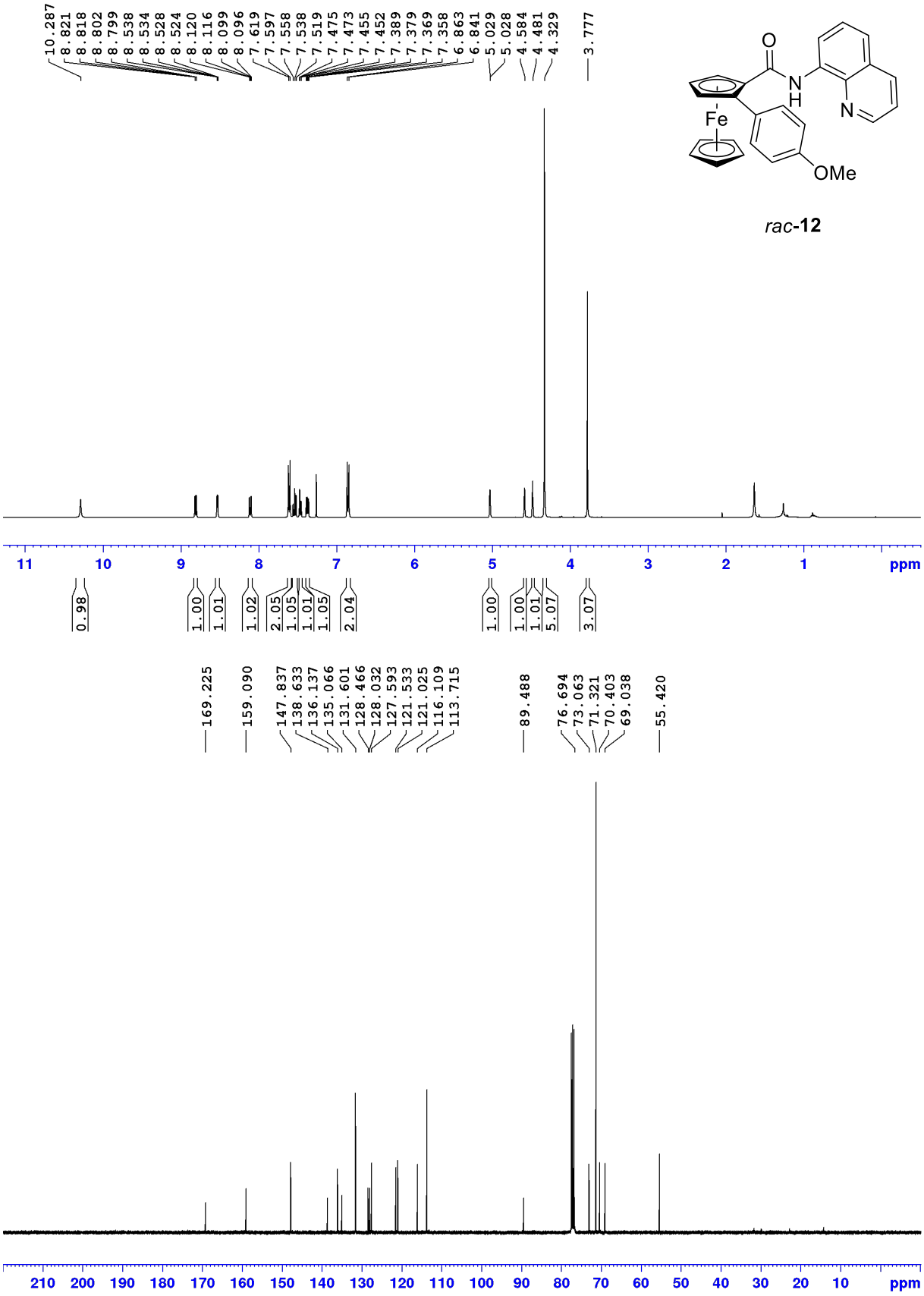

Figure S12. ^{1}H (400 MHz) and ^{13}C (100.6 MHz) NMR Spectra of *N*-[2-(1-Benzyl-1*H*-1,2,3-triazol-4-yl)-propan-2-yl]-2-(4-methylphenyl)ferrocenoylamide (*rac*-**13**) in $CDCl_3$

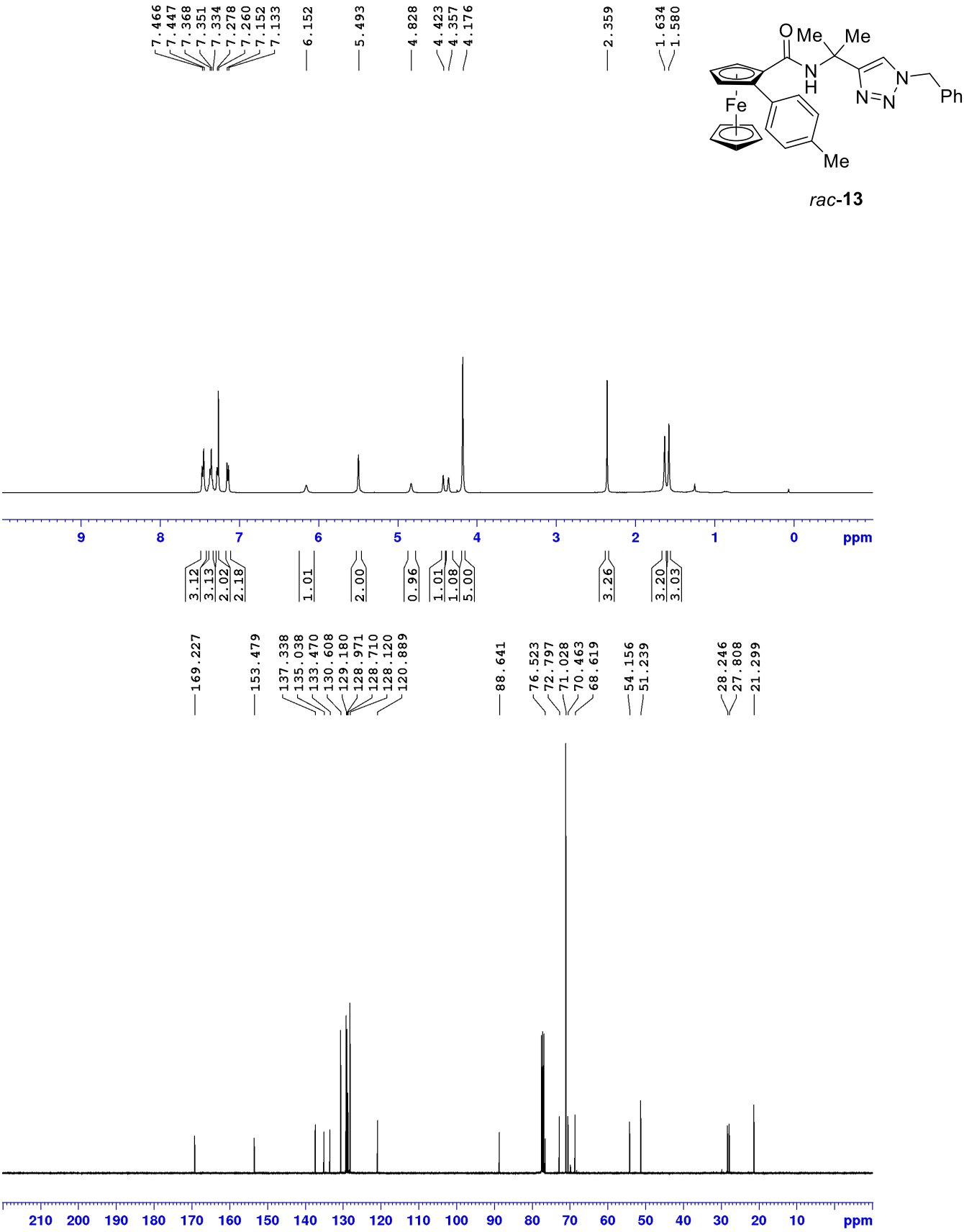

Figure S13. ^{1}H (400 MHz) and ^{13}C (100.6 MHz) NMR Spectra of *N*-[2-(1-Benzyl-1*H*-1,2,3-triazol-4-yl)-propan-2-yl]-2-(4-trifluormethylphenyl)ferrocenoylamide (*rac*-**14**) in $CDCl_3$

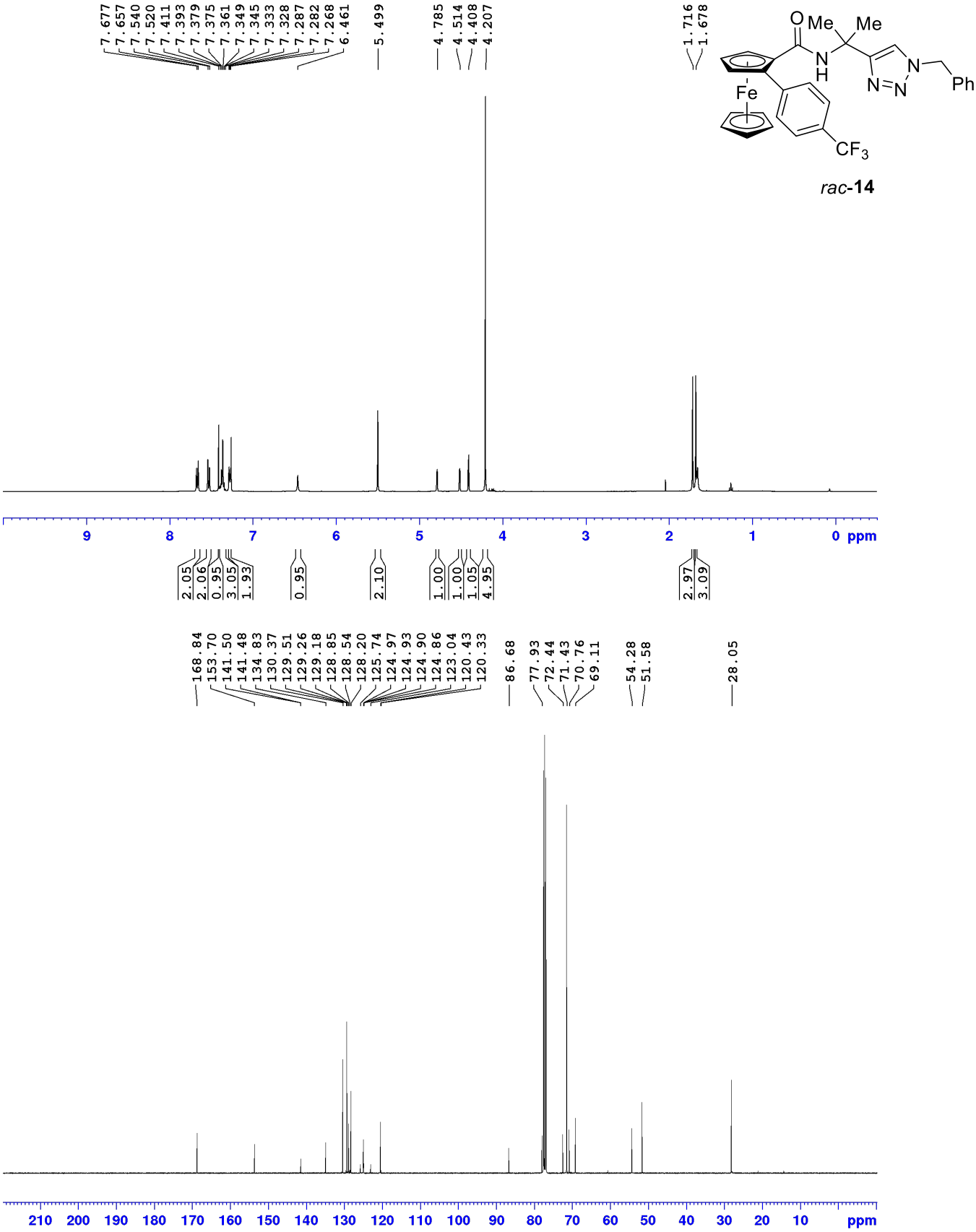

Figure S15. ^{19}F (376.5 MHz) NMR Spectrum of *rac*-**14** in $CDCl_3$

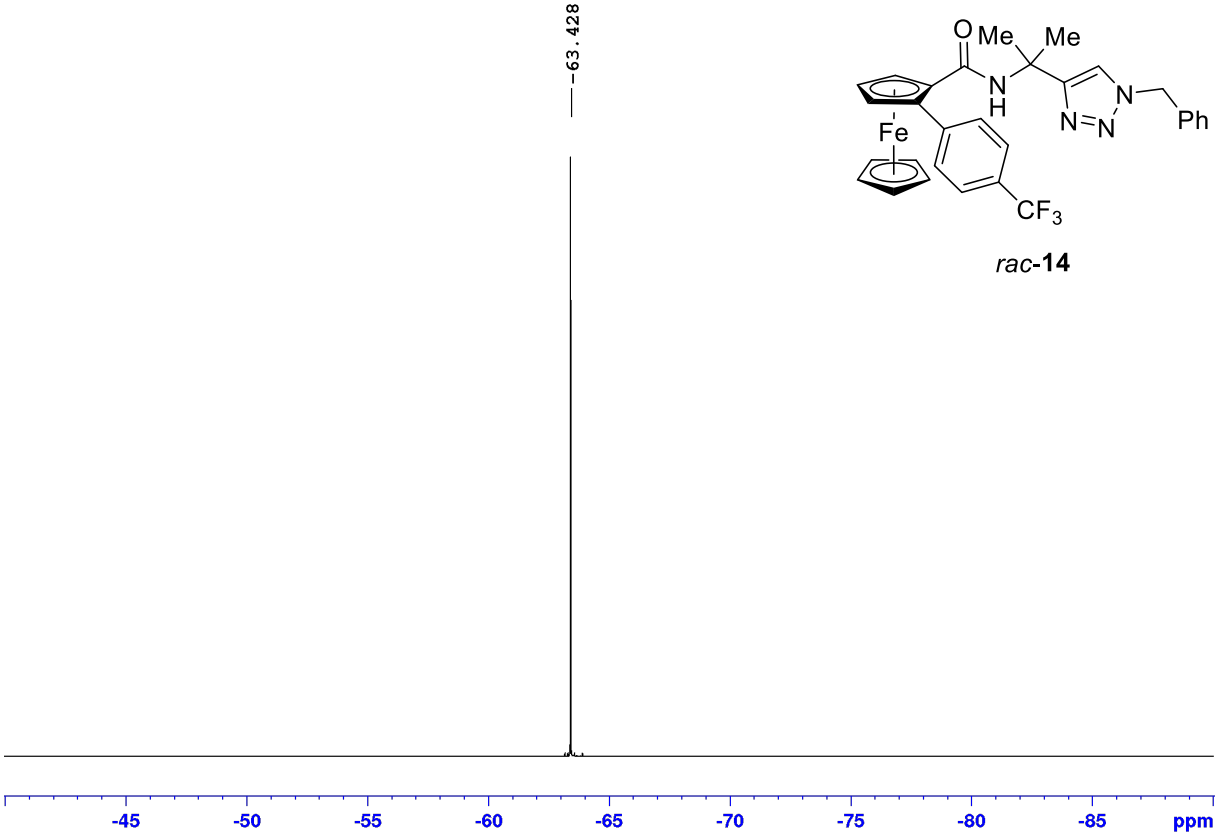

Figure S16. ^{1}H (400 MHz) and ^{13}C (100.6 MHz) NMR Spectra of *N*-[2-(1-Benzyl-1*H*-1,2,3-triazol-4-yl)-propan-2-yl]-2-(4-methoxyphenyl)ferrocenoylamide (*rac*-**15**) in $CDCl_3$

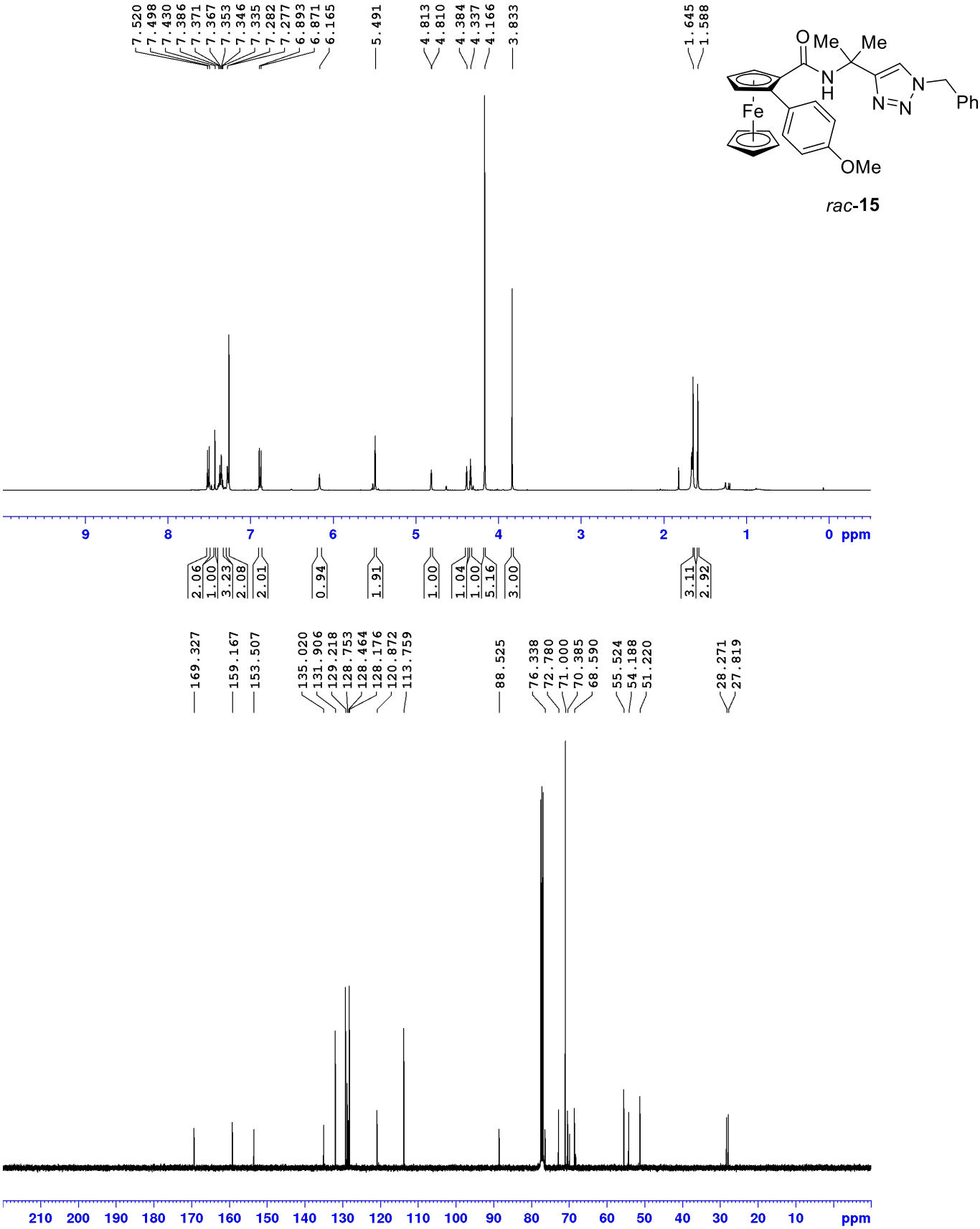

Figure S17. ^{1}H (400 MHz) and ^{13}C (100.6 MHz) NMR Spectra of *N*-(8-Quinolinyl)-2-methylferrocenoylamide (*rac*-**18**) in $CDCl_3$

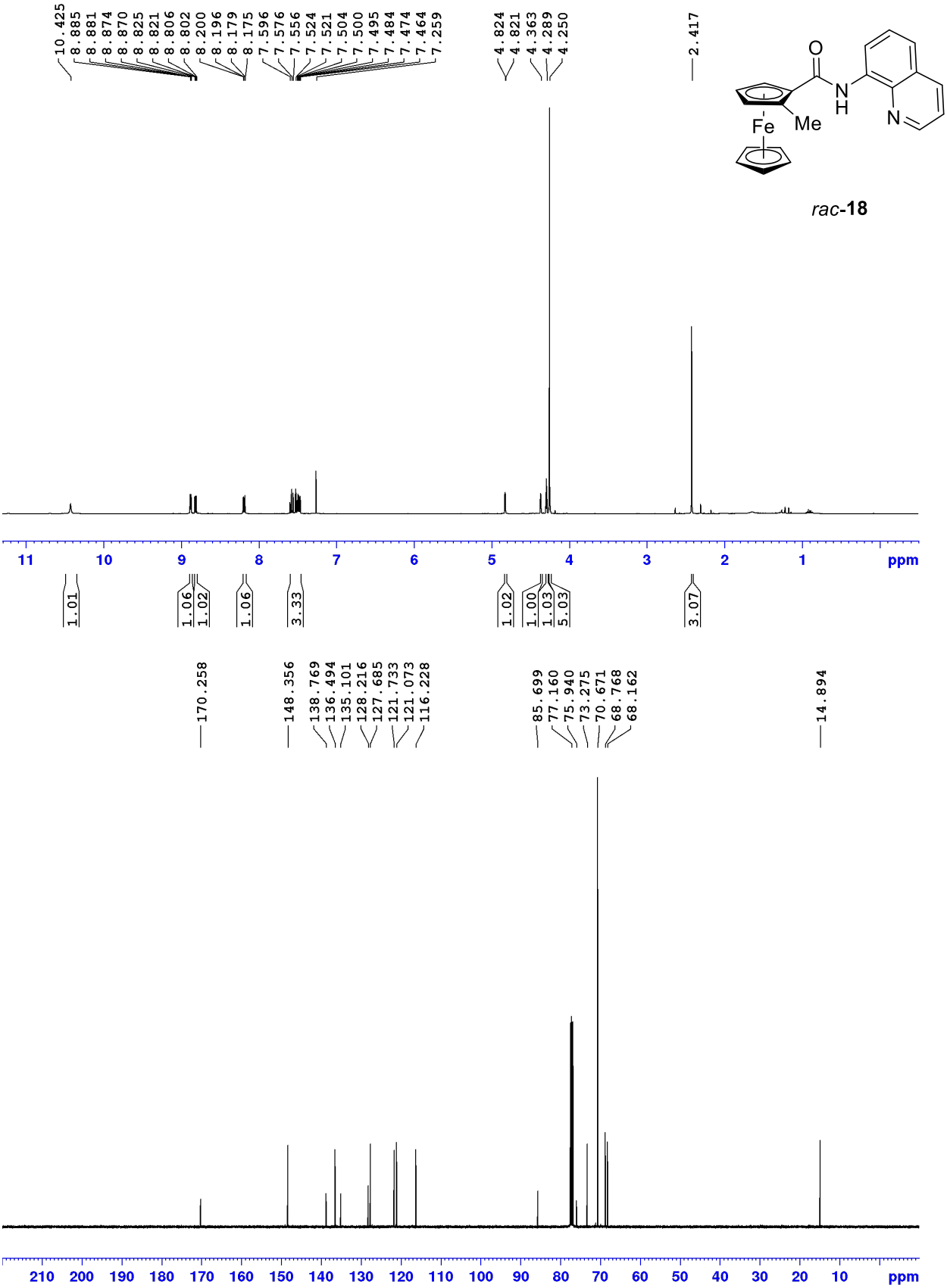

Figure S18. ^{1}H (400 MHz) and ^{13}C (100.6 MHz) NMR Spectra of *meso-N,N'*-Bis(8-quinolinyl)-1,1'-diferrocenoylamide (**20**) in $CDCl_3$

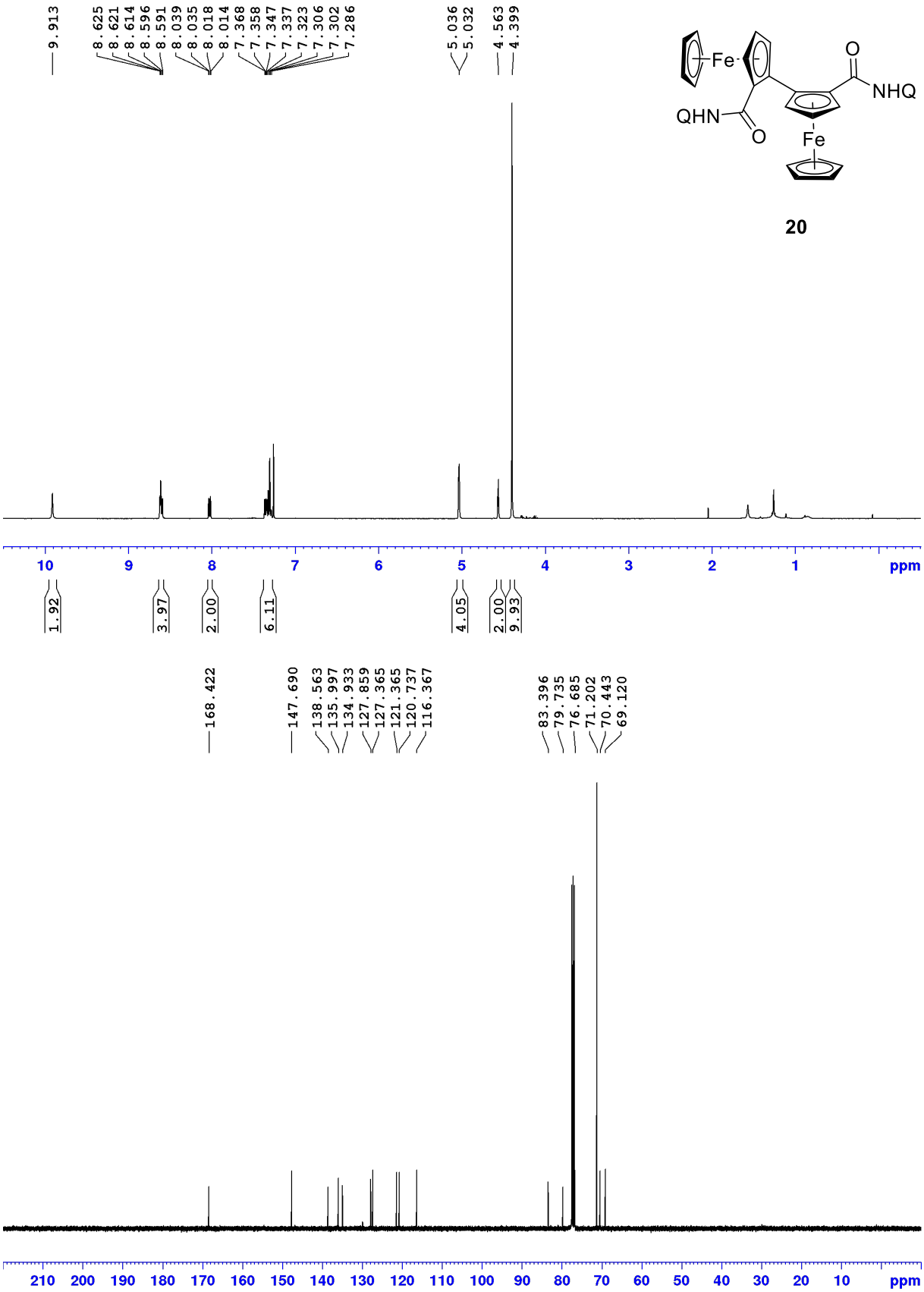

Figure S19. ^{1}H (400 MHz) and ^{13}C (100.6 MHz) NMR Spectra of *N*,*N*'-Bis(8-quinolinyl)-2-methyl-1,1'-diferrocenoylamide (*rac*-**21**) in $CDCl_3$

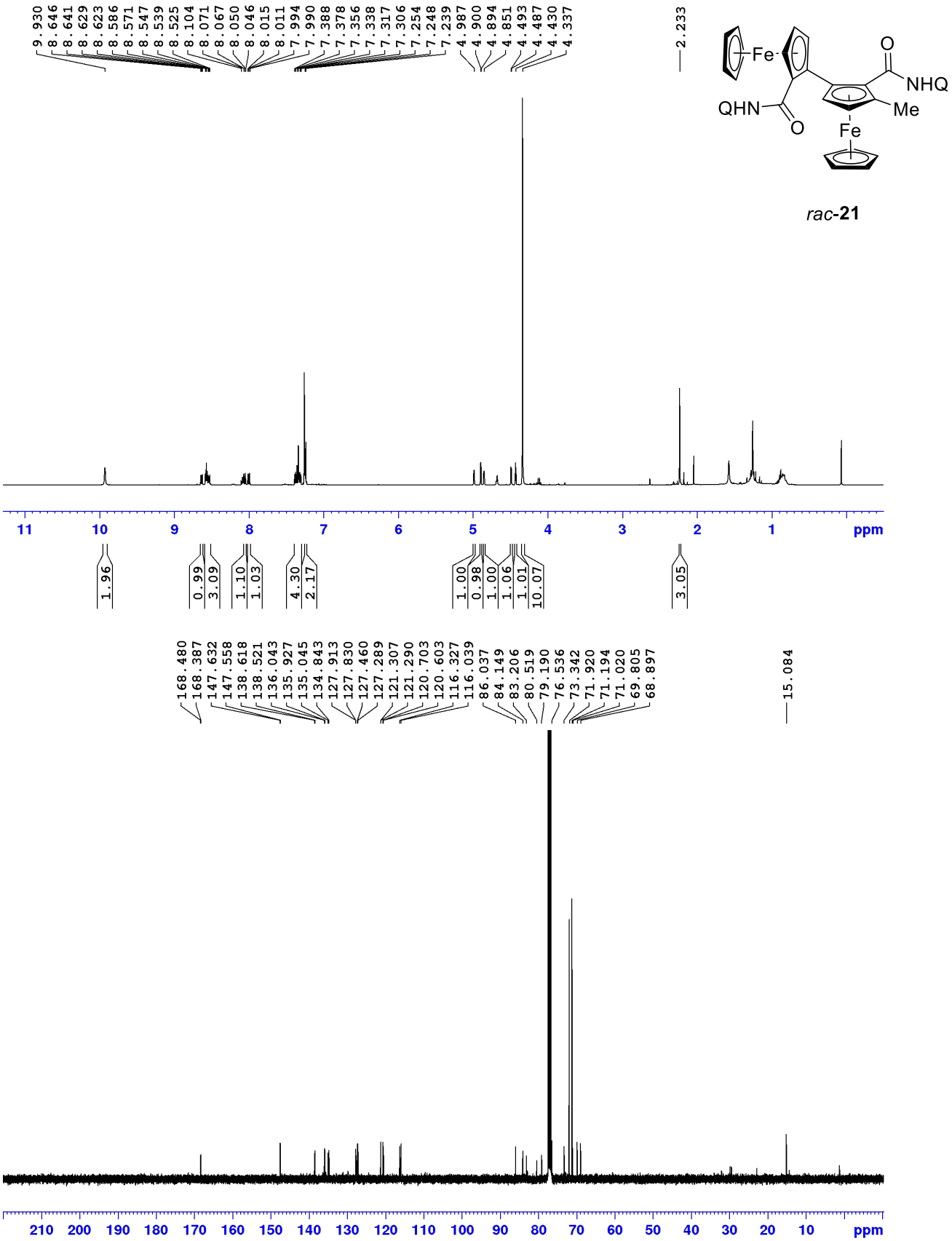

Figure S20. ^{1}H (400 MHz) and ^{13}C (100.6 MHz) NMR Spectra of *N*-[2-(1-Benzyl-1*H*-1,2,3-triazol-4-yl)-propan-2-yl]-2-ethylferrocenoylamide (*rac*-**15**) in $CDCl_3$

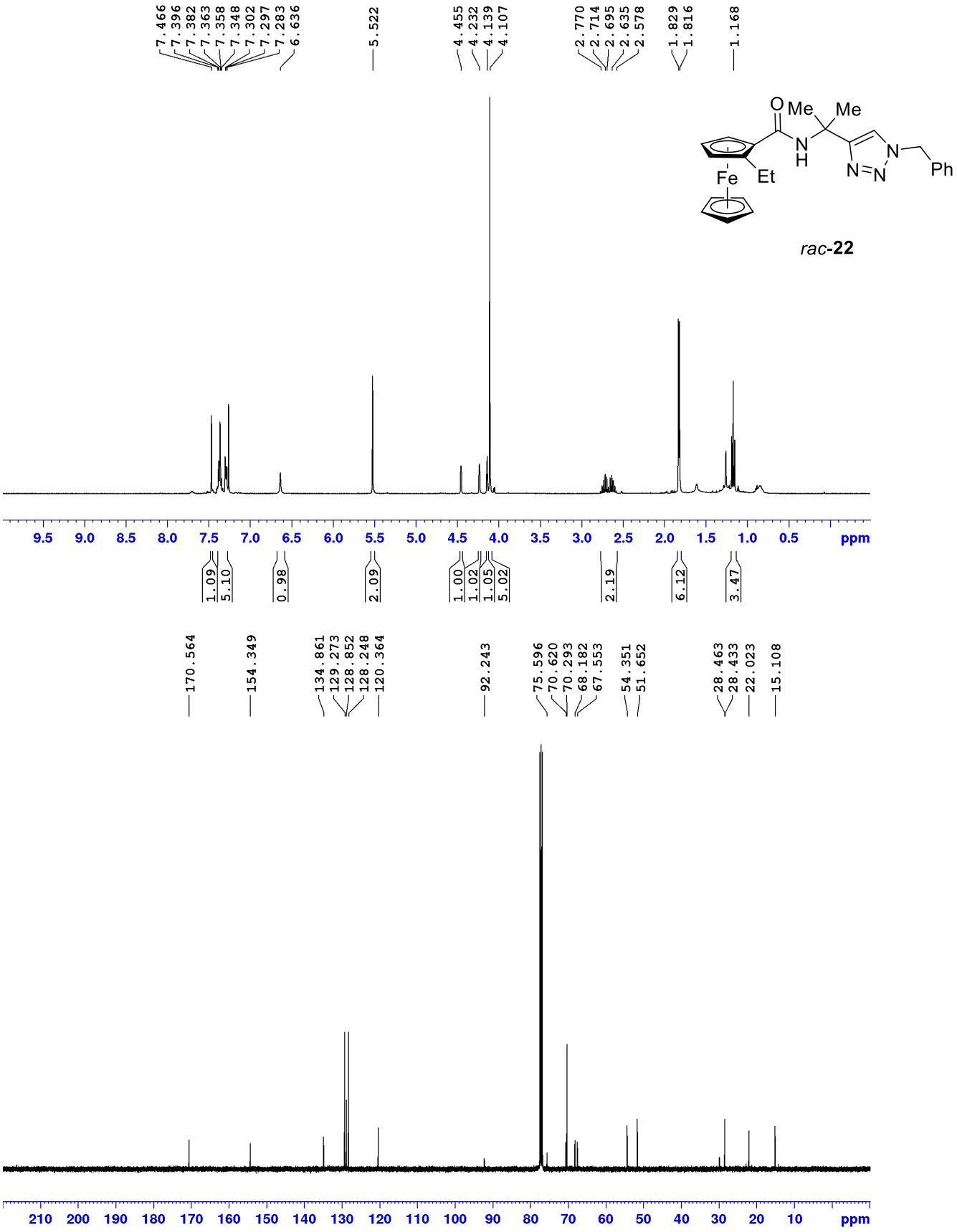

Figure S21. ^{1}H (400 MHz) and ^{13}C (100.6 MHz) NMR Spectra of *N*-[2-(1-Benzyl-1*H*-1,2,3-triazol-4-yl)propan-2-yl]-2,5-dimethylferrocenoylamide (**25**) in $CDCl_3$

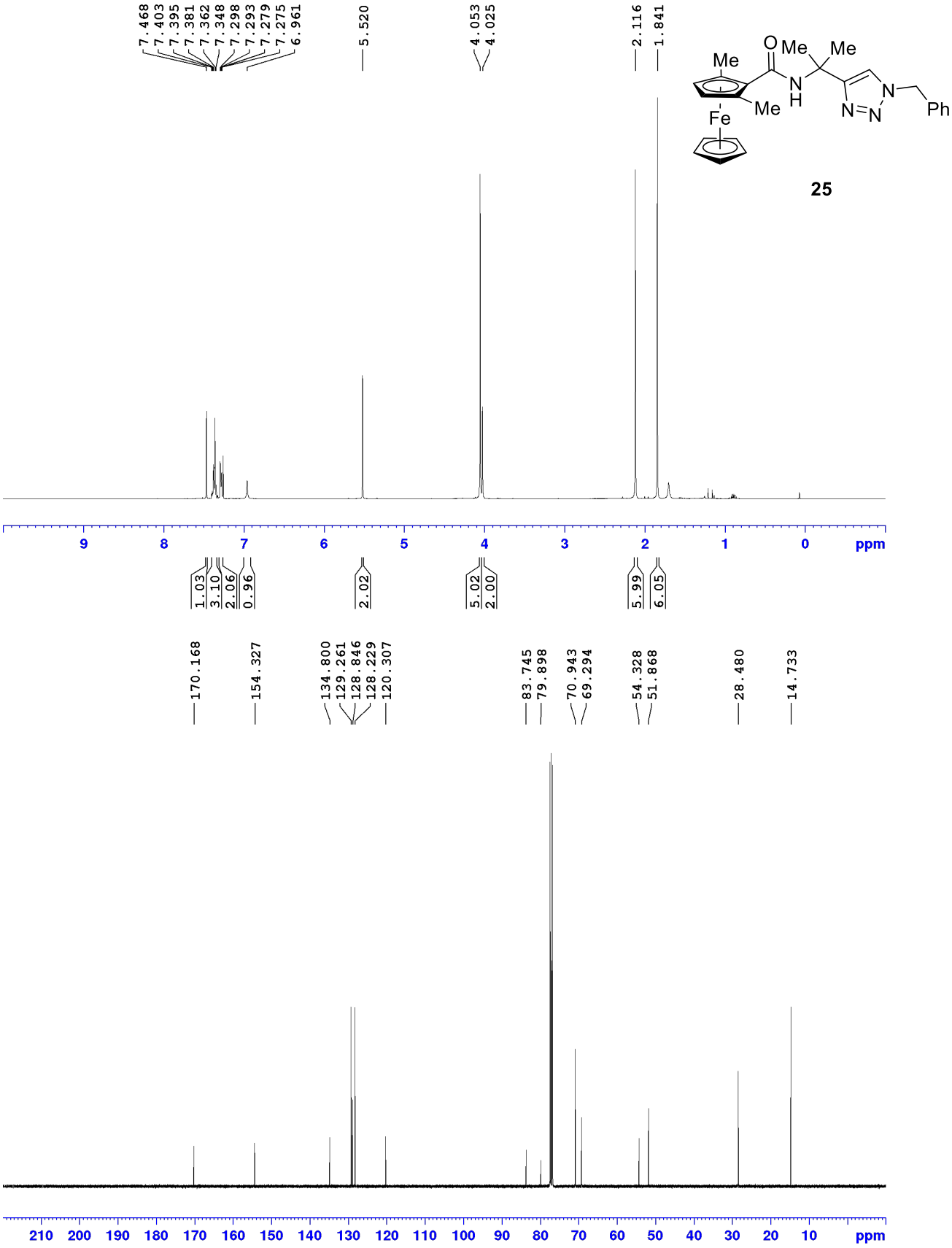

Figure S22. ^{1}H (400 MHz) and ^{13}C (100.6 MHz) NMR Spectra of (*S*)-*N*-[2-(4-Benzyloxazolin-2-yl)-2-propanyl]ferrocenoylamide [(*S*)-**26**] in $CDCl_3$

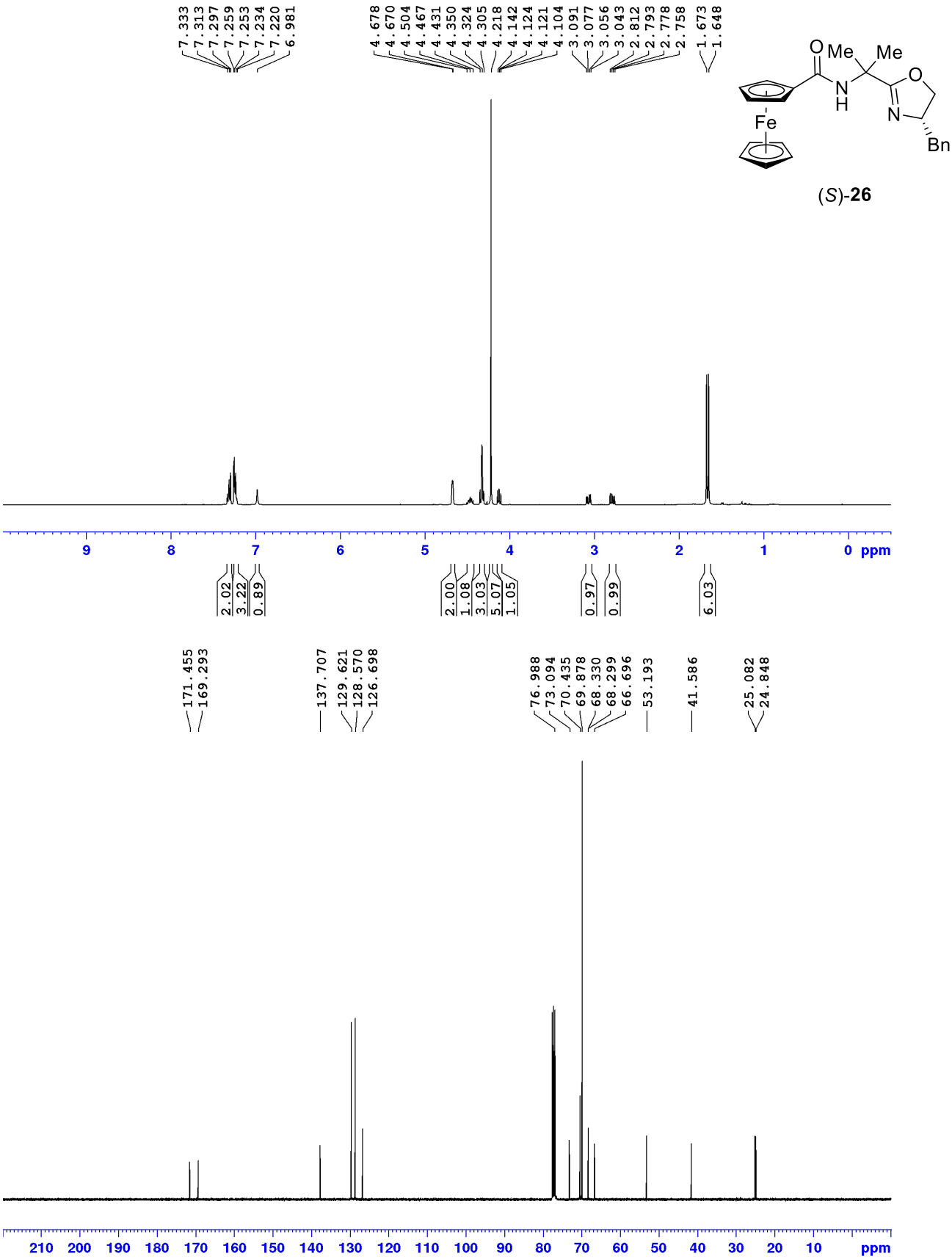

Figure S23. ^{1}H (400 MHz) and ^{13}C (100.6 MHz) NMR Spectra of (S,S_p)-N-[2-(4-Benzyl-2-oxazolinyl)propan-2-yl]-2-methylferrocenoylamide [(S,S_p)-**27**] in $CDCl_3$

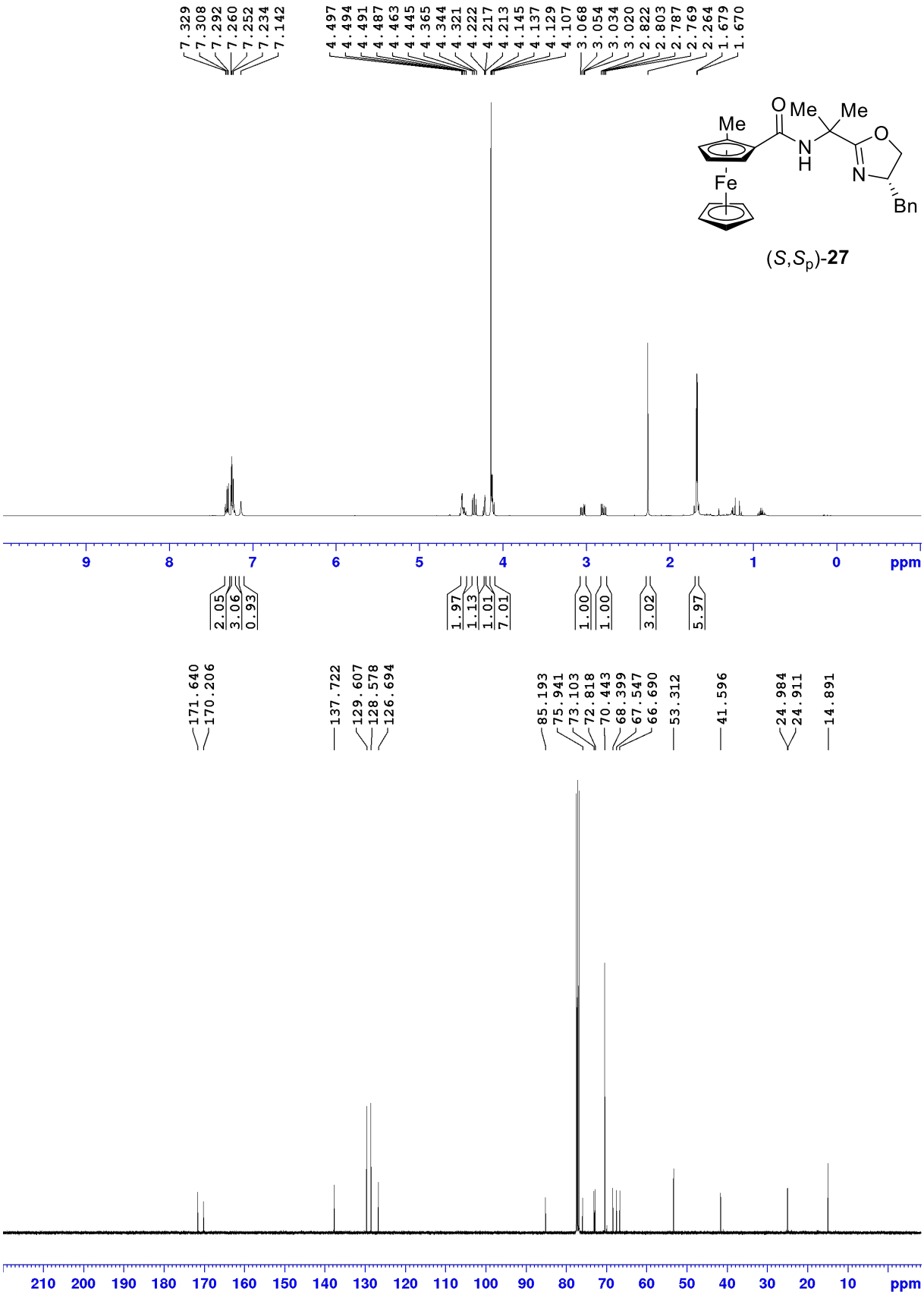

Figure S24. ^{1}H (400 MHz) and ^{13}C (100.6 MHz) NMR Spectra of (*S*)-*N*-[2-(4-Benzyl-2-oxazolinyl)propan-2-yl]-2,5-dimethylferrocenoylamide [(*S*)-**28**] in $CDCl_3$

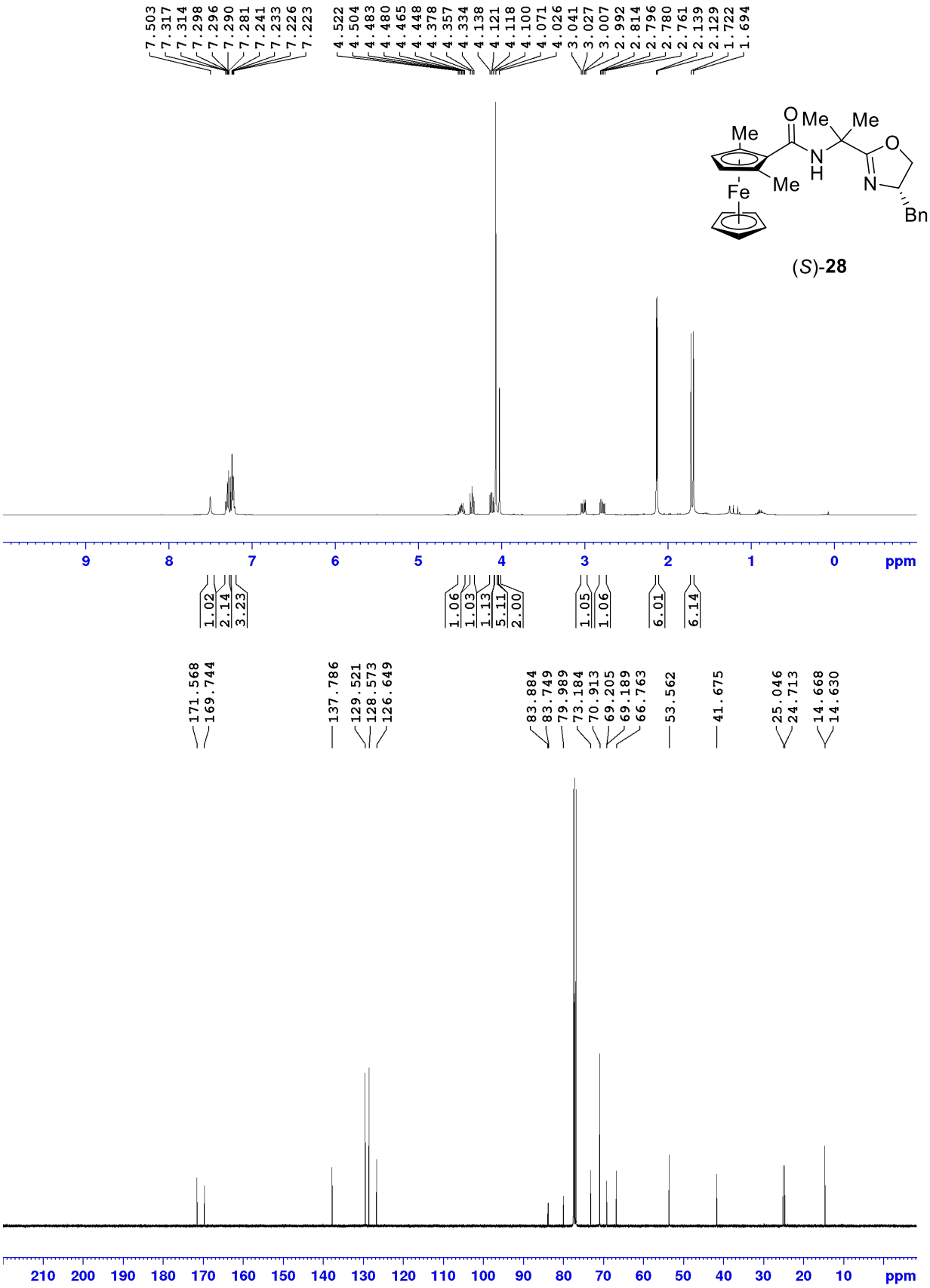

Figure S25. ^{1}H (400 MHz) and ^{13}C (100.6 MHz) NMR Spectra of 2-(4-Methylphenyl)ferrocene-1-carbonitrile (*rac*-**30**) in $CDCl_3$

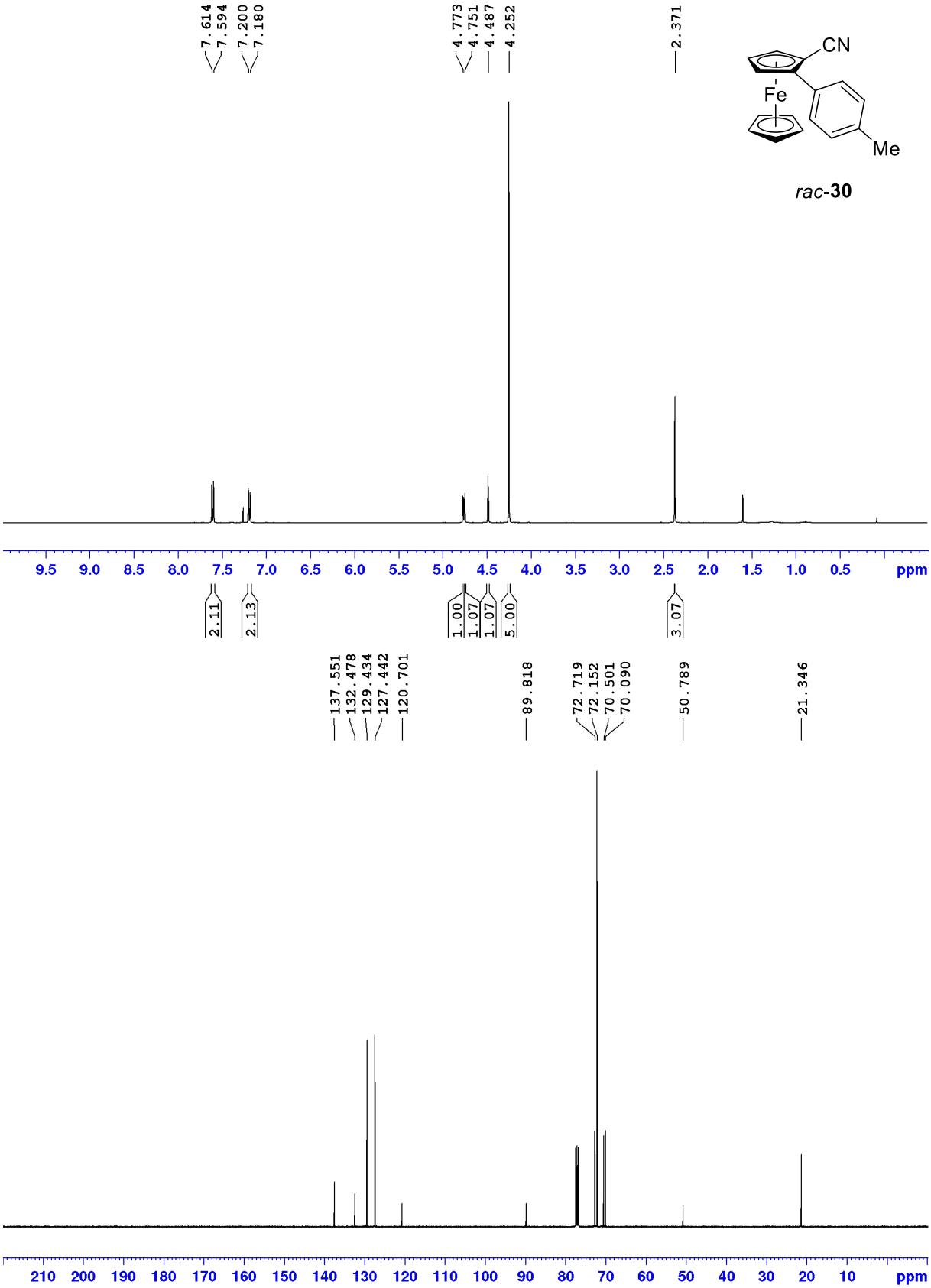

Enantioselective Phenylation of 1 and 5:

Table 3, entry 2; GP; **1** (90 mg, 0.25 mmol), $ZnBr_2$·TMEDA (256 mg, 0.75 mmol), (*R*,*R*)-Chiraphos (16 mg, 0.04 mmol) and PhMgBr (3M in Et_2O, 0.5 mL, 1.5 mmol); column chromatography (25 x 2.5 cm, petroleum ether/ethyl acetate 6:1) afforded (+)-**3** (103 mg, 0.24 mmol, 95 %) as an orange oil.

$[\alpha]_D^{20}$: +31.6 (*c* = 1.0, $CHCl_3$ for 43% *ee*). Analytical data: see *rac*-**3**. The enantiomeric excess was determined by HPLC with a Daicel Chiralcel OD-H column, hexane/2-propanol as eluent with a flow rate of 0.5 mL/min, λ = 254 nm, *t*(minor) = 30.72 min, *t*(major) = 36.63 min.

Figure S26. Chromatogram for *rac*-**3**

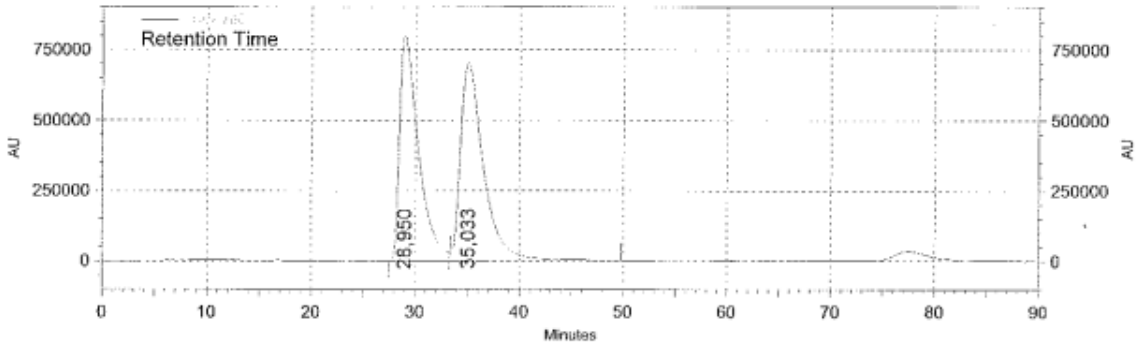

Det 166 Results

Time	Area	Area %	Height	Height %
28,950	100883888	48,46	799741	53,31
35,033	107313388	51,54	700569	46,69
Totals	208197276	100,00	1500310	100,00

Figure S27. Chromatogram for (+)-**3**

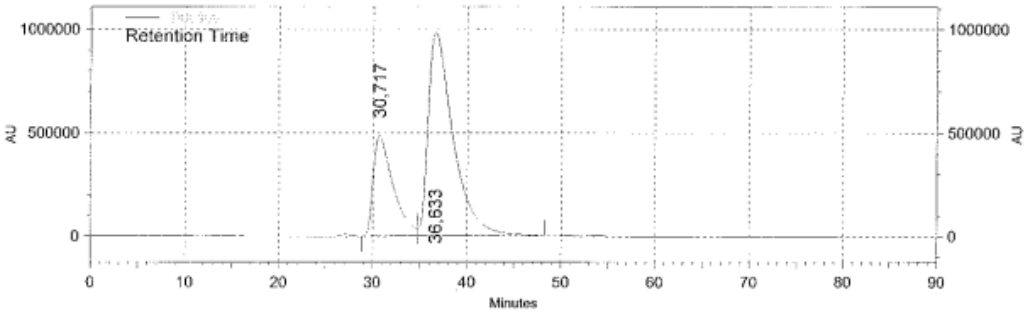

Det 166 Results

Time	Area	Area %	Height	Height %
30,717	71431498	28,29	484423	32,98
36,633	181057742	71,71	984369	67,02
Totals	252489240	100,00	1468792	100,00

Table 3, entry 3; GP; **5** (86 mg, 0.2 mmol), $ZnBr_2$·TMEDA TMEDA (205 mg, 0.6 mmol), (*R*,*R*)-Chiraphos (13 mg, 0.03 mmol) and PhMgBr (3M in Et_2O, 0.4 mL, 1.2 mmol); column chromatography (25 x 2.5 cm, petroleum ether/ethyl acetate 6:1) affored (+)-**6** (90 mg, 0.18 mmol, 89 %) as an orange solid.

$[\alpha]_D^{20}$: +2.7 (*c* = 1.0, $CHCl_3$ for 46% *ee*). Analytical data: see *rac*-**6**. The enantiomeric excess was determined by HPLC with a Daicel Chiralcel OD-H column, hexane/2-propanol as eluent with a flow rate of 0.5 mL/min, λ = 254 nm, *t*(minor) = 48.22 min, *t*(major) = 54.48 min.

Figure S28. Chromatogram for *rac*-**6**:

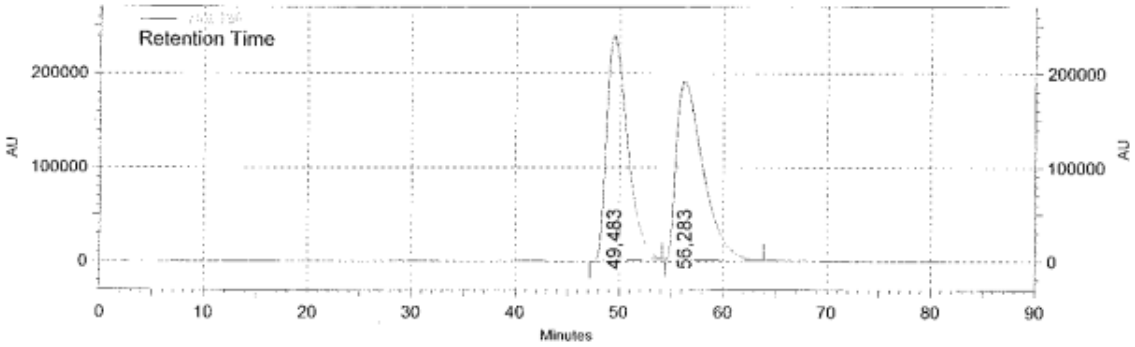

Det 166 Results

Time	Area	Area %	Height	Height %
49,483	33636439	50,18	239910	55,68
56,283	33398360	49,82	190950	44,32
Totals	67034799	100,00	430860	100,00

Figure S29. Chromatogram for (+)-**6**:

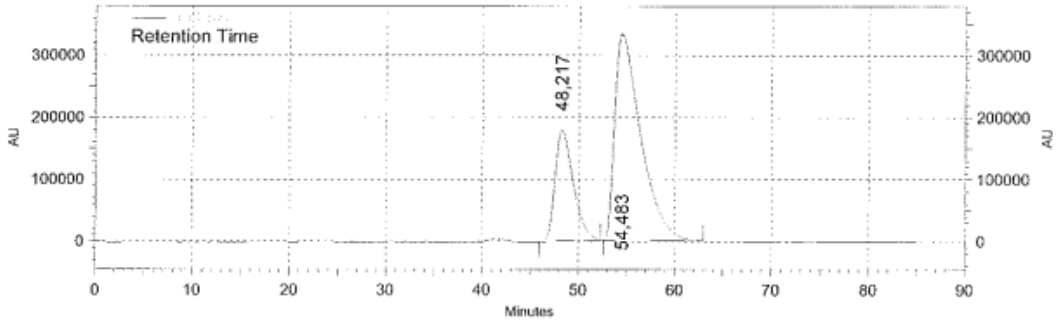

Det 166 Results

Time	Area	Area %	Height	Height %
48,217	23405155	27,17	179668	34,91
54,483	62731874	72,83	334987	65,09
Totals	86137029	100,00	514655	100,00